LANGMUIR Article
Cite This: Langmuir 2017, 33, 13423-13429 pubs.acs.org/Langmuir

Supported Lipid Bilayers with Phosphatidylethanolamine as the Major Component

Anne M. Sendecki,[†] Matthew F. Poyton,[†] Alexis J. Baxter,[†] Tinglu Yang,[†] and Paul S. Cremer*[,†,‡]

[†]Department of Chemistry and [‡]Department of Biochemistry and Molecular Biology, Pennsylvania State University, University Park, Pennsylvania 16802, United States

Supporting Information

ABSTRACT: Phosphatidylethanolamine (PE) is notoriously difficult to incorporate into model membrane systems, such as fluid supported lipid bilayers (SLBs), at high concentrations because of its intrinsic negative curvature. Using fluorescence-based techniques, we demonstrate that having fewer sites of unsaturation in the lipid tails leads to high-quality SLBs because these lipids help to minimize the curvature. Moreover, shorter saturated chains can help maintain the membranes in the fluid phase. Using these two guidelines, we find that up to 70 mol % PE can be incorporated into SLBs at room temperature and up to 90 mol % PE can be incorporated at 37 °C. Curiously, conditions under which three-dimensional tubules project outward from the planar surface as well as conditions under which domain formation occurs can be found. We have employed these model membrane systems to explore the ability of Ni^{2+} to bind to PE. It was found that this transition metal ion binds 1000-fold tighter to PE than to phosphatidylcholine lipids. In the future, this platform could be exploited to monitor the binding of other transition metal ions or the binding of antimicrobial peptides. It could also be employed to explore the physical properties of PE-containing membranes, such as phase domain behavior and intermolecular hydrogen bonding.

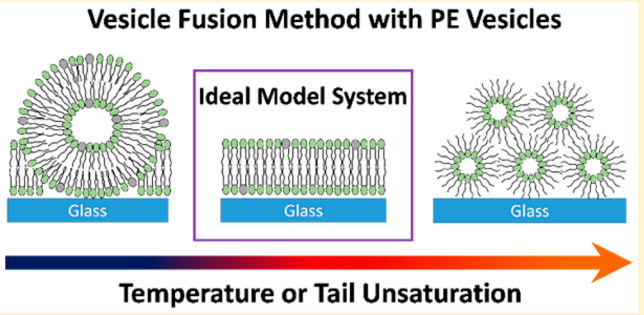

INTRODUCTION

The head group structure of phospholipids is one of the main factors that determines their biological role and function. The zwitterionic phospholipids, phosphatidylethanolamine (PE) and phosphatidylcholine (PC), have almost identical structures, except for the methylation of the amine (Figure 1A), which leads to significant differences in their respective behaviors.[1,2] PE can act as a hydrogen bond donor, and its amine can be deprotonated, giving it unique interactions not only with other bilayer components[3] but also with ions and molecules from the bulk solution.[4] PE also has an intrinsic curvature, which affects its role within biological membranes as a stabilizer of membrane proteins.[5] Despite these unique interactions, PC has historically been used as the predominate phospholipid in model system studies and has even been used as a substitute for PE or treated as interchangeable with PE.[6−8] This has unfortunately limited the information available about the biophysical properties of PE.

PE is the second most abundant phospholipid in eukaryotic cells, representing 25 mol % of the overall lipid content, and can comprise up to 45 mol % of phospholipids in the nervous tissue.[9,10] It is the most abundant phospholipid in many bacteria, primarily Gram-negative bacteria, where it makes up 70−80 mol % of membrane lipids.[1,11] It has various biological functions, including serving as a protein cofactor,[11,12] and is required for proper folding of certain proteins.[7] It has also been shown to bind to copper ions, which can enhance the rate of lipid oxidation.[4] Because of its biological importance and abundance, creating model lipid bilayer systems that contain physiologically relevant concentrations of PE would be very advantageous. Moreover, making supported lipid bilayers (SLBs) with PE lipids affords the traditional benefits of heterogeneous assays, such as compatibility with a variety of surface-sensitive techniques. However, creating fluid SLBs with physiologically relevant concentrations of PE lipids in the presence of PC lipids has been a challenge. For example, Hamai et al. demonstrated that using 20 mol % or more of a PE lipid, 1,2-dioleoyl-*sn*-glycero-3-phosphoethanolamine (DOPE), in supported bilayers also containing 1,2-dioleoyl-*sn*-glycero-3-phosphocholine (DOPC), led to incomplete bilayer formation.[13]

Forming stable SLBs via the vesicle fusion method depends upon the intrinsic curvature of the individual lipids.[13] Many phospholipids, such as PC, have two tails and an overall cylindrical shape and can readily form planar bilayers (Figure 1B). Typical intrinsic curvature values for PC are close to 0 nm^{-1}. In fact, the intrinsic curvature value for DOPC is −0.1 nm^{-1}[14] and those for 1-palmitoyl-2-oleoyl-*sn*-glycero-3-phosphocholine (POPC)[14] as well as 1,2-dilauroyl-*sn*-glycero-3-phosphocholine (DLPC) are 0.0 nm^{-1}.[15] By contrast, PE has a

Received: July 4, 2017
Revised: October 14, 2017
Published: November 9, 2017

DOI: 10.1021/acs.langmuir.7b02323
Langmuir 2017, 33, 13423−13429

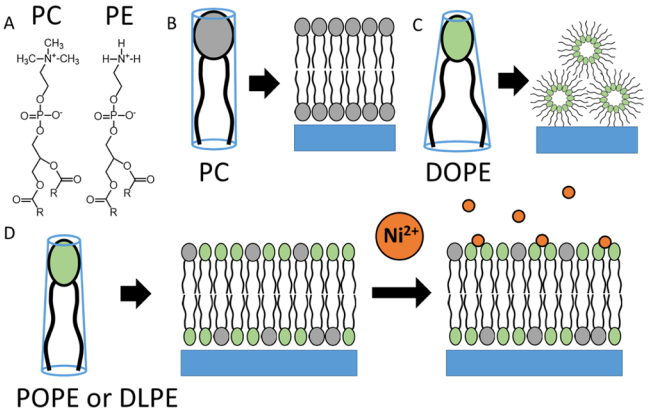

Figure 1. Comparison of PC and PE lipids with schematic representations of the resulting SLB constructs and assays. (A) Head group structures of PC and PE. (B) Cylindrical PC lipids form fluid SLBs. (C) Lipids with a high negative curvature such as DOPE form hexagonal phase structures. (D) PE lipids with less curvature, such as POPE or DLPE, can form fluid SLBs when mixed with PC lipids, allowing for Ni^{+} binding assays to be performed (PE asymmetry in the membrane is discussed on page S2 in the Supporting Information section).

significantly smaller head group, giving it a more conical shape (Figure 1C). The intrinsic curvature is -0.4 nm^{-1} for DOPE[14] and -0.3 nm^{-1} for both 1-palmitoyl-2-oleoyl-*sn*-glycero-3-phosphoethanolamine (POPE)[14] and 1,2-dilauroyl-*sn*-glycero-3-phosphoethanolamine (DLPE).[16]

The negative curvature of PE lipids leads to a unique phase behavior that is not observed with PC lipids. Specifically, the addition of double bonds into the alkyl chains leads to a conically shaped molecule that will not readily assemble into a planar sheet (lamellar phase) because of the strain introduced by the intrinsic curvature of each lipid (Figure 1C, right).[13] Instead, a hexagonal phase is often favored, in which the head groups face toward the center and the tails are splayed outward. PE lipids undergo a transition from the lamellar to the hexagonal phase at a temperature that is dependent on the length of the tails and the number of sites of unsaturation.[17] For example, DOPE, which has two 18:1 lipid tails, has a hexagonal phase transition temperature, T_h, of 10 °C. Therefore, it is not possible to form a homogeneous SLB at room temperature with physiologically relevant amounts of DOPE. By contrast, POPE (16:0, 18:1) and DLPE (12:0, 12:0), which contain 1 and 0 sites of unsaturation, respectively, have gel-to-liquid phase transition temperatures (T_m) of 25 and 29 °C[18] and T_h temperatures of 71 and 131 °C,[19] respectively. As such, they are significantly better candidates. Herein, we show that fluid SLBs containing up to 70 mol % POPE in POPC or 50 mol % DLPE in DLPC can be made at room temperature. Moreover, fluid SLBs containing 90 mol % of these PE lipids in PC can be assembled at 37 °C. Finally, a nickel-binding fluorescence assay was performed with 50 mol % POPE in the bilayer (Figure 1D). It was found that Ni^{2+} bound to POPE with an apparent dissociation constant, K_D, of 0.38 mM. This value is several orders of magnitude lower than for POPC, indicating a tighter binding of the transition metal with PE lipids than that with PC lipids.[20]

MATERIALS AND METHODS

Lipid Vesicle Preparation. Large unilamellar vesicles were made by the freeze–thaw extrusion method.[21,22] Briefly, the lipids were mixed at the desired ratio in chloroform and then placed under vacuum for 1.5 h. The lipid film was rehydrated to a density of 1 mg/mL in an aqueous buffer containing 10 mM dibasic sodium phosphate and 100 mM NaCl at pH 7.4 and sonicated for 20 min. The lipid suspensions were then subjected to 10 freeze–thaw cycles and extruded through a filter with 100 nm pores. Vesicles containing 70 mol % PE or higher were extruded at ∼40 °C to ensure that they were in the fluid phase. All vesicles were used within 7 days of preparation.

Temperature Control. For experiments conducted at 37 °C, a programmable temperature controller (VWR) was employed directly on the microscope stage to heat the glass slide, which served as the underlying substrate for the bilayer. The temperature was monitored on the underside of the slide. Vesicles were added to preheated poly(dimethylsiloxane) (PDMS) wells on the glass slide and incubated while being heated and then rinsed with heated 18.2 MΩ water. The well was finally covered with a glass coverslip to prevent evaporation, and the temperature was allowed to re-equilibrate for 20 min before being used to ensure temperature homogeneity. For experiments conducted at 23 °C, vesicles were added to wells, incubated, and rinsed with 18.2 MΩ water at room temperature.

Fluorescence Recovery after Photobleaching (FRAP). FRAP[23,24] experiments were carried out with a Nikon Eclipse TE-2000-U inverted microscope through a 10× objective. A 532 nm 300 mW solid-state laser (Dragon Lasers) was used to bleach the Texas Red 1,2-dihexadecanoyl-*sn*-glycero-3-phosphoethanolamine, triethylammonium salt (TR-DHPE) with a power averaging 5 mW for 1 s at the sample. The average diameter of the laser beam was 20 μm, yielding 0.016 mW/μm^2 as the power per unit area. The average fluorescence intensity of the spot was analyzed over time as the bleached fluorophores diffused out and unbleached fluorophores took their place. Images were initially taken every 3 s, until the fluorescence in the bleached area no longer visually appeared to change, and then switched to every 30 or 60 s to minimize photobleaching. The fluorescence of the bleached spot was normalized to an unbleached reference spot, and the percentage recovery was plotted over time

$$F(t) = \frac{F_t - F_0}{1 - F_0}$$

where F_t is the normalized fluorescence at time t and F_0 is the normalized fluorescence at $t = 0$. The results were fit to a single exponential

$$y = A(1 - e^{-bx})$$

where A corresponds to the mobile fraction (i.e., percentage of the bilayer able to recover) and b was used to calculate the diffusion coefficient, D (how quickly the bilayer recovered)

$$\tau_{1/2} = \frac{\ln(2)}{b} \qquad D = \frac{w^2}{4r_{1/2}} \times \gamma$$

where w is the diameter of the laser beam and γ is the correction factor determined by the beam shape and the depth of bleaching, with a value of 0.88.[23]

Nickel Titration Measurements. PDMS/glass microfluidic devices were fabricated according to procedures described in the Supporting Information section, *Microfluidic Device Fabrication* (page S7) and in previous publications.[25] Briefly, 10 μL of the desired vesicle solution was introduced into each microfluidic channel and incubated for 30 min to form SLBs. Buffer containing 10 mM Tris and 100 mM NaCl at pH 8.5 was used throughout the experiment. Buffer with increasing concentrations of $NiCl_2$ was introduced through plastic tubing, with each solution flowing continuously for at least 1 h to reach the steady state before measuring the fluorescence with a Nikon Eclipse TE-2000-U inverted microscope through a 4× objective. Then, the tubing at the inlet was removed, drained of solution, and the next solution was drawn through; then, the tubing was reinserted. The fluorescence intensity was measured with a line function in MetaMorph. The background fluorescence was subtracted from the average fluorescence of each channel and was normalized to the initial

DOI: 10.1021/acs.langmuir.7b02323
Langmuir 2017, 33, 13423–13429

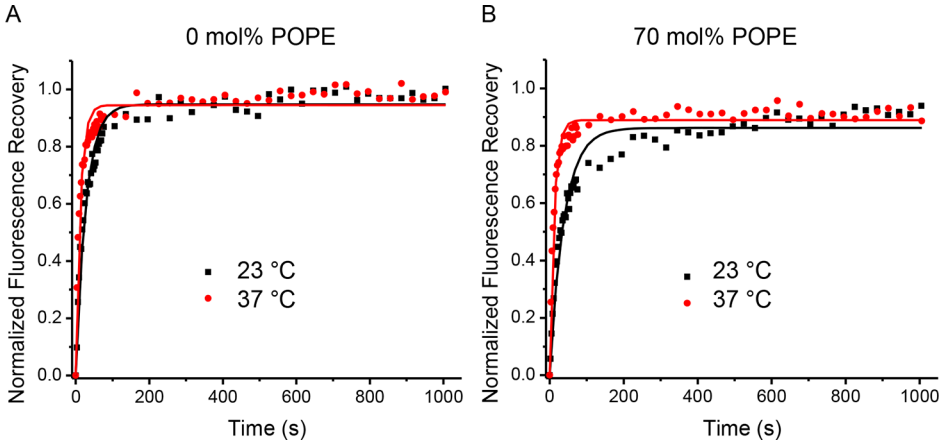

Figure 2. FRAP curves for two lipid compositions at 23 and 37 °C. (A) Bilayers were formed with 0 mol % POPE, 99.5 mol % POPC, and 0.5 mol % TR-DHPE. (B) Bilayers were formed with 70 mol % POPE, 29.5 mol % POPC, and 0.5 mol % TR-DHPE. The solid lines are single exponential fits to the data. For additional fits, see Figure S1.

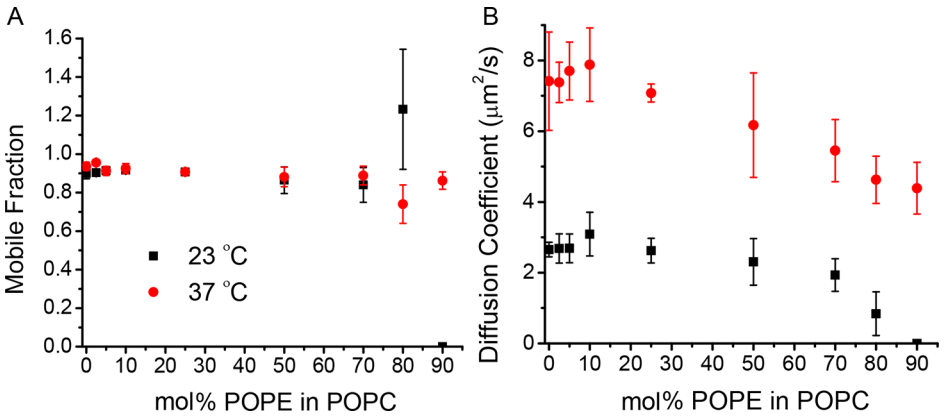

Figure 3. Diffusivity of SLBs containing POPE and POPC analyzed by FRAP at 23 and 37 °C. (A) Mobile fraction. (B) Diffusion coefficient.

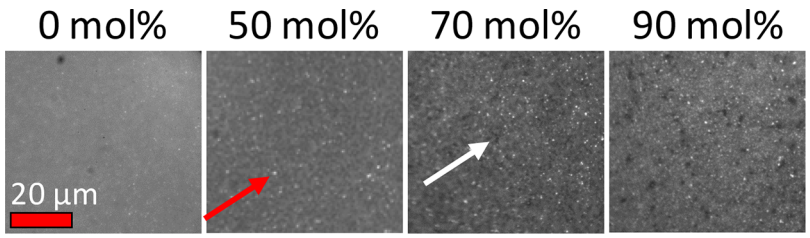

Figure 4. Fluorescent images of POPE-containing SLBs at 100× magnification at room temperature. As the amount of POPE was increased, the concentration of defects increased. The bright spot indicated by the red arrow in the 50 mol % image was putatively from a three-dimensional structure, and the dark patch indicated by the white arrow in the 70 mol % image was a liquid-ordered phase domain. For other mol % POPE SLBs, see Figure S4.

fluorescence before the addition of $NiCl_2$. Because of significant collisional quenching of all bilayers at millimolar concentrations, the fluorescence change from POPC bilayers was subtracted as described in the Supporting Information section, *Subtraction of Collisional Quenching and Fitting to a Langmuir Isotherm* on page S23.

RESULTS AND DISCUSSION

POPE Bilayers at 23 °C. In the first set of experiments, we investigated the SLBs formed by the vesicle fusion method at 23 °C that contained various concentrations of POPE in POPC. All membranes contained 0.5 mol % TR-DHPE to visualize the SLBs by epifluorescence microscopy. The SLBs were quantitatively analyzed by FRAP (Figure 2). Figure 2 shows the representative FRAP curves for supported bilayers made with (A) 99.5 mol % POPC and (B) 70 mol % POPE and 29.5 mol % POPC at both 23 and 37 °C. Without POPE, a single exponential fit agrees reasonably well with the fluorescence recovery curves at both temperatures (discussion of double exponential fits are provided in Figures S1 and S2, which compares the bilayer and monolayer diffusion). At 70 mol % POPE, however, the data diverged more significantly from a single exponential fit at room temperature, reflecting a decrease in homogeneity, but was improved at 37 °C, as will be discussed later.

FRAP results for POPE/POPC compositions ranging from 0 to 90 mol % PE are summarized in Figure 3. Both the mobile fraction of dye molecules in the membrane (A) and the associated diffusion constants (B) are provided. When mixed

DOI: 10.1021/acs.langmuir.7b02323
Langmuir 2017, 33, 13423−13429

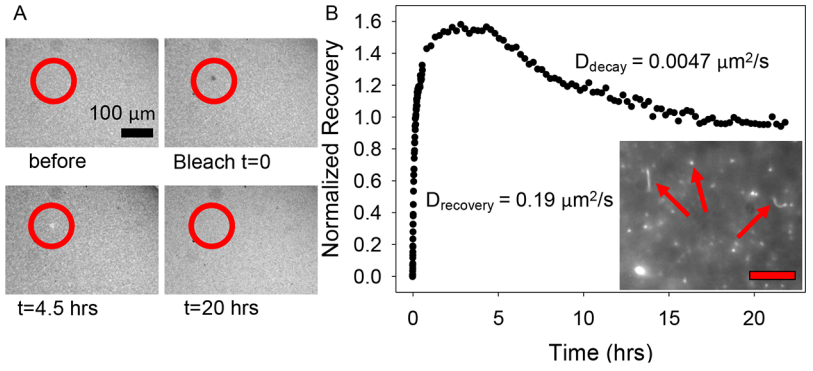

Figure 5. Extended-time FRAP study of 80 mol % POPE bilayers. (A) Fluorescence images of the bilayer before bleaching, just after bleaching, after 4.5, and after 20 h. The bleached area is highlighted with a red circle in each image. (B) Corresponding FRAP recovery curve. The $D_{recovery}$ values were calculated from the initial rise (t = 0−5 h) and D_{decay} values were calculated from the subsequent decrease (t > 5 h) in the fluorescence intensity. D_{decay} was calculated using an exponential decay curve, as described in the Supporting Information section, *Fitting Exponential Decay* on page S4. The inset fluorescent image shows tubules approximately 5 μm above the surface. The red arrows point to tubules. The longer looking ones are bent and therefore more fully in the focal plane. Others are bright spots from tubules extending through the focal plane, as can be seen in Movie S1. The scale bar is 10 μm.

with POPC, which has a T_m of −2 °C,[18] SLBs could be formed with an approximately 90% mobile dye fraction for PE concentrations as high as 70 mol % at both 23 and 37 °C. Moreover, the dye molecules displayed diffusion constants near to or above 2 $\mu m^2/s$ with up to 70 mol % POPE. Together, these metrics demonstrate that the supported bilayers were in the fluid phase with up to 70 mol % POPE.

Under closer inspection, it was possible to see small defects in bilayers with higher POPE concentrations, such as unruptured vesicles, and these increased in number with increasing amounts of PE (Figure 4). The fluorescence images show bright spots, which are three-dimensional structures protruding from the surface. Underwater tapping mode atomic force microscopy (AFM) data also confirmed that the three-dimensional structures were formed with increasing amounts of POPE (Figure S3). By contrast, there was little, if any, evidence for holes or similar defects by either AFM or protein adsorption measurements, in which a fluorescently labeled protein was used as a probe for exposed regions of the glass surface (Figure S4).

At 70 mol % POPE, higher magnification revealed phase domain formation with characteristic domain sizes on the order of 1 μm in length (Figures S5 and S6). This was expected, as Cannon et al. have shown that the melting transition for vesicles composed of 70 mol % POPE and 30 mol % POPC is just below the room temperature at 22 °C.[4,26] These domains recovered with a measurable diffusion coefficient (Figure S1 shows the double exponential fit) and therefore are not in the gel phase but rather represent liquid-ordered domains.

With 80 mol % POPE, the bilayers behaved more unusually, as reflected in their FRAP and attenuated total reflection infrared spectroscopy (ATR-IR) data (Figure S7). The data at 80 mol % showed an apparent mobile fraction above 1 (Figure 3A). Such an anomalous behavior arose because the dye molecule, TR-DHPE, was sequestered into small areas where it was highly concentrated, resulting in self-quenching.[27] When the bilayer was bleached, self-quenching was reduced, which allowed recovery above 100% in the 4.5 h image (Figure 5A). The over recovery occurred because the 80 mol % SLBs were inhomogeneous. Not only do they have domains, but high magnification revealed that three-dimensional tubules extended out from the bilayer (the inset in Figure 5B shows a snapshot and a full movie is in the Supporting Information). These were highly curved structures with diameters below the diffraction limit of light. The tubules were anchored to the SLB at one end and extended several microns above the surface. The three-dimensional structures observed by AFM with lower concentrations of POPE (Figure S3) may have been precursors to the tubules seen with 80 mol % POPE. Because POPE can form highly curved structures,[1] it was presumed to be enriched in the inner leaflet of the tubules. This idea was supported by ATR-IR data (Table S1), which showed considerably less POPE than that predicted at the surface, as the tubules extend beyond the penetration depth of the ATR-IR measurement (~0.3 μm).

TR-DHPE is also known to prefer highly curved structures because of its bulky head group,[28] and the tubules were clearly visible against the SLB fluorescence from below (Figure 5B, inset). During FRAP, both the bilayer and the tubules were bleached simultaneously. As shown in Figure 5B, the initial increase and the subsequent leveling off of the recovery curve were fit to extract the mobile fraction and diffusion coefficient reported in Figure 3, as this most closely reflects the diffusion of the lipids in a two-dimensional bilayer with domain structures. However, when monitored over much longer time periods, the fluorescence began to decrease again (20 h image in Figure 5A). In fact, the fluorescence attenuated by about one-third over a time scale of approximately 15 h (see the Supporting Information section, *Fitting Exponential Decay* on page S4 for fitting details). This lower diffusion constant most likely reflected the diffusion of the dye along the tubules in the z-direction. As the tubules extended nearly 20 μm in the z-direction above the SLB (see Movie S1), well outside of the microscope's depth of view (~0.5 μm), the dye needed to diffuse back to the surface through the tubules above to be visualized. Indeed, the tubules acted as a sink for the dyes, requiring significantly more dye and longer times to reestablish self-quenching.

At 90 mol % POPE, the mobile fraction and diffusion coefficient were both zero at 23 °C (Figure 3). Under these circumstances, the level of fluorescence intensity from the surface was quite low. In fact, it does not appear that the surface was well-covered with the bilayer material and that the residual fluorescence arose from adhered vesicles. We also attempted to form bilayers with 99 mol % POPE and 1 mol % of a variety of

DOI: 10.1021/acs.langmuir.7b02323
Langmuir 2017, 33, 13423−13429

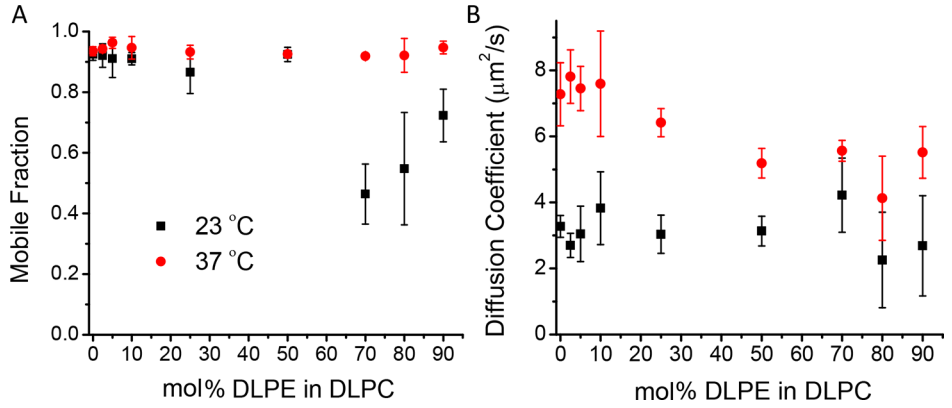

Figure 6. Properties of SLBs with mixed DLPE and DLPC lipids at room temperature and at physiological temperature. (A) Mobile fraction and (B) diffusion coefficient data.

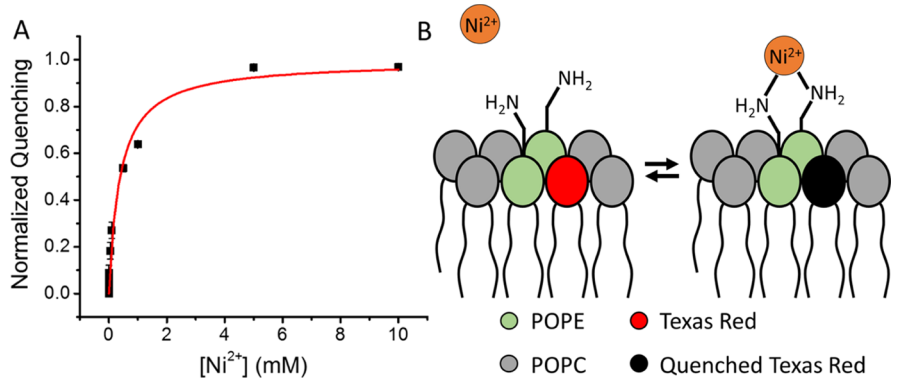

Figure 7. (A) Ni^{2+}-binding titration curve measured at 23 °C in 10 mM Tris buffer at pH 8.5. (B) Representation of Ni^{2+}-binding to two deprotonated PE head groups. Bivalent binding is expected at this density of PE.[4]

fluorophores. This was not possible because of poor incorporation of the fluorophores into the bilayer under these conditions (Supporting Information section, *Making 100 mol % PE SLBs* on page S17).

POPE Bilayers at 37 °C. Selecting the tails for PE lipids that have less intrinsic negative curvature clearly increased the amount of PE that could be incorporated into fluid SLBs at room temperature compared to previous reports.[13] However, membranes formed with POPE lipids still have a relatively high T_m value. As such, one should expect to encounter issues with fluidity at higher PE concentrations when working at room temperature. Raising the temperature to 37 °C, which is above T_m of POPE, should allow fluidity to be restored to the SLBs. Qualitatively, the visible defects and domains that appeared at room temperature were no longer evident or greatly reduced at 37 °C (Figure S8). Moreover, with 80 and 90 mol % PE, the bilayers started out with defects that annealed over time (Figure S9). The mobile fractions of the 37 °C bilayers were all at least slightly higher than the corresponding ones at room temperature (red data points, Figure 3). The only exception to this was 80 mol % POPE, which had a mobile fraction above 1 at 23 °C because of bilayer inhomogeneities. At 37 °C, they no longer showed over recovery, and no tubules or domains were observed under these conditions. ATR-IR confirmed that the lipid composition of the SLBs matched the nominal composition up to 90 mol % (Table S1).

DLPE Bilayers. To further explore the effects of unsaturation in lipid tails and corroborate the results seen with POPE SLBs, we conducted FRAP experiments using DLPE, which eliminated all double bonds and had a gel-to-liquid phase transition temperature comparable to POPE.[18] Generally, results seen with DLPE were similar to those seen for POPE (Figures 6 and S10, which provide FRAP data and fluorescent images, respectively). The SLBs maintained high mobility and diffusion coefficients with up to 50 mol % PE at 23 °C, whereas higher mol % PE exhibited defects and irreproducibility (Figure S11). At 37 °C, the behavior of the DLPE bilayers was similar to that of POPE, showing increased mobile fractions, less visible defects, and brighter fluorescence (Figure 6, red points and Figure S12). In fact, the mobile fraction for 90 mol % DLPE bilayers was 95% at 37 °C. As such, fluid SLBs with a high mobile fraction for either POPE or DLPE can be made when working near physiological temperatures. The diffusion coefficients of both POPE and DLPE bilayers showed a temperature dependence, which was independent of the fluorophore used (Figure S13).

Ni^{2+} Binding Assay. PE-containing bilayers can be used to investigate a variety of physical properties with PE lipids. Unlike PC, the primary amine of PE can be deprotonated and therefore can form metal−ligand binding complexes. Previously, it has been shown that Cu^{2+} forms complexes with lipid head groups by directly binding to amines on phosphatidylserine[29,30] as well as with PE.[4] Specifically, the primary amine from PE can directly bind to transition metals to form a metal coordination complex in its deprotonated form. As such, we hypothesized that other transition metals from the Irving-Williams series should also be able to bind.[31,32] To test this hypothesis, we performed experiments with $NiCl_2$ using SLBs

DOI: 10.1021/acs.langmuir.7b02323
Langmuir 2017, 33, 13423−13429

in a microfluidic device, where increasing concentrations of Ni^{2+} were introduced above an SLB. Figure S14 shows fluorescent images in the absence and presence of Ni^{2+}. When Ni^{2+} was bound to PE, it quenched the nearby fluorophores through an energy transfer mechanism.[33] This provided a direct measure of Ni^{2+}-binding to the SLB. Figure 7a shows the Ni^{2+}-binding curve for a bilayer containing 50 mol % POPE at room temperature, with a fitted K_D value of 0.38 mM (see Figure S15 and Supporting Information section, *Subtraction of Collisional Quenching and Fitting to a Langmuir Isotherm* on page S23 for fitting details). This is in stark contrast to Ni^{2+}-binding to a PC head group, which has been reported to be 1.2 M,[20] a value that was more than a factor of 3000 weaker. Because deprotonation of the amine was a crucial step in binding (Figure 7b), the binding curve was measured at pH 8.5, which increased the available binding sites but should not affect the intrinsic K_D value.[4] This experiment represents a clear but simple demonstration of the differences in the behavior for membranes containing significant concentrations of PE compared to membranes that contain just PC.

CONCLUSIONS

PE can be employed in SLB studies despite its negative curvature. PE lipids have often been classified as nonbilayer lipids because of their conical shape,[1] though they can be incorporated into unilamellar gel phases or liquid-ordered phases.[34,35] Indeed, many studies use PE only to introduce membrane curvature, ignoring possible effects of hydrogen bonding. By incorporating PE into planar SLBs, it is possible to focus on head group interactions instead and minimize the curvature effects. PE is both a hydrogen-bond donor and acceptor, whereas PC is only a hydrogen-bond acceptor. This capability opens up a host of potential interactions both with other membrane components and with molecules or proteins in the bulk solution.

It is known that PE can hydrogen bond with the phosphate and carbonyl groups of the neighboring PE lipids[3,36] and has been predicted to hydrogen bond with other lipids such as phosphatidylglycerol (PG).[37] PE can also form hydrogen bonds with water, causing differences in hydration as well as allowing water molecules to bridge neighboring lipids.[38] Such intrabilayer hydrogen bonds could direct the organization of lipid domains.[3] As demonstrated herein, PE can be used to form domains of either liquid-ordered or gel (see *DLPE Bilayers* in the Supporting Information) phases in two component systems, where presumably the PE-rich domains contain many intermolecular hydrogen bonds. Similarly, these hydrogen-bonding networks likely extend to PE/PG interactions, impacting the organization of PG.[39] Indeed, Seeger et al. used AFM to study the phase transitions of individual leaflets of 3:1 PE/PG bilayers.[40] With the capability to study PE-enriched SLBs, it should be possible to gain a better understanding of the role of PE in two or more component systems that exhibit phase separation.

There are many basic physiological properties of biological membranes that exploit PE rather than PC lipids. We expect that these model systems will be extremely useful for measuring the affinity of small molecules which bind to the membranes containing PE lipids. One example involves the use of PE-enriched SLBs to study the effects of antimicrobial peptides. Antimicrobial peptides are an important developing area of research as antibiotic resistant bacteria are on the rise.[41] The effectiveness of antimicrobial peptides is dependent upon lipid composition,[42,43] and a simple model system is needed to elucidate the individual contributions of different lipids. PE is the major component of many bacterial membranes, such as *Escherichia coli*. As such, it is vital to study the interactions of PE with antimicrobial peptides to understand the binding and transbilayer penetration of peptides to formulate improved peptides for biomedical uses. PE-containing SLBs provide a direct route to systematic studies of these and other interactions.

ASSOCIATED CONTENT

Supporting Information

The Supporting Information is available free of charge on the ACS Publications website at DOI: 10.1021/acs.langmuir.7b02323.

Additional materials and methods; FRAP curves fit to double exponentials; characterization of domains; fluorescence images of POPE SLBs under different magnifications, formed at different temperatures, and the annealing seen at 37 °C; FRAP data, fluorescent images, and interpretation for DLPE/DLPC SLBs; temperature dependence of the diffusion coefficient with another fluorophore; summary table of ATR-IR data of POPE SLBs; discussion of 100 mol % PE SLBs; and details on subtraction of collisional quenching (PDF)

Three-dimensional tubules observed with 80 mol % SLBs (AVI)

AUTHOR INFORMATION

Corresponding Author

*E-mail: psc11@psu.edu.

ORCID

Paul S. Cremer: 0000-0002-8524-0438

Notes

The authors declare no competing financial interest.

ACKNOWLEDGMENTS

This work was funded by the Office of Naval Research (N00014-14-1-0792) and the Penn State MRSEC, Center for Nanoscale Science, under the award NSF DMR-1420620. The authors thank Simou Sun for help with the FRAP experiments performed.

REFERENCES

(1) Dowhan, W. Molecular Basis for Membrane Phospholipid Diversity: Why Are There So Many Lipids? *Annu. Rev. Biochem.* **1997**, *66*, 199−232.

(2) Brown, M. F. Soft Matter in Lipid−Protein Interactions. In *Annual Review of Biophysics*; Dill, K. A., Ed.; Annual Reviews: Palo Alto, 2017; Vol. *46*, pp 379−410.

(3) Boggs, J. M. Lipid intermolecular hydrogen bonding: influence on structural organization and membrane function. *Biochim. Biophys. Acta* **1987**, *906*, 353−404.

(4) Poyton, M. F.; Sendecki, A. M.; Cong, X.; Cremer, P. S. Cu^{2+} Binds to Phosphatidylethanolamine and Increases Oxidation in Lipid Membranes. *J. Am. Chem. Soc.* **2016**, *138*, 1584−1590.

(5) Slater, S. J.; Kelly, M. B.; Taddeo, F. J.; Ho, C.; Rubin, E.; Stubbs, C. D. The Modulation of Protein Kinase C Activity by Membrane Lipid Bilayer Structure. *J. Biol. Chem.* **1994**, *269*, 4866−4871.

(6) Petrache, H. I.; Dodd, S. W.; Brown, M. F. Area per lipid and acyl length distributions in fluid phosphatidylcholines determined by 2H NMR spectroscopy. *Biophys. J.* **2000**, *79*, 3172−3192.

DOI: 10.1021/acs.langmuir.7b02323
Langmuir 2017, 33, 13423−13429

(7) Bogdanov, M.; Sun, J.; Kaback, H. R.; Dowhan, W. A Phospholipid Acts as a Chaperone in Assembly of a Membrane Transport Protein. *J. Biol. Chem.* **1996**, *271*, 11615−11618.
(8) Keller, S. L.; Bezrukov, S. M.; Gruner, S. M.; Tate, M. W.; Vodyanoy, I.; Parsegian, V. A. Probability of Alamethicin Conductance States Varies with Nonlamellar Tendency of Bilayer Phospholipids. *Biophys. J.* **1993**, *65*, 23−27.
(9) Vance, J. E. Thematic review series: Glycerolipids. Phosphatidylserine and phosphatidylethanolamine in mammalian cells: two metabolically related aminophospholipids. *J. Lipid Res.* **2008**, *49*, 1377−1387.
(10) Deleault, N. R.; Piro, J. R.; Walsh, D. J.; Wang, F.; Ma, J.; Geoghegan, J. C.; Supattapone, S. Isolation of phosphatidylethanolamine as a solitary cofactor for prion formation in the absence of nucleic acids. *Proc. Natl. Acad. Sci. U.S.A.* **2012**, *109*, 8546−8551.
(11) Morein, S.; Andersson, A.-S.; Rilfors, L.; Lindblom, G. Wild-type *Escherichia coli* Cells Regulate the Membrane Lipid Composition in a Window between Gel and Non-lamellar Structures. *J. Biol. Chem.* **1996**, *271*, 6801−6809.
(12) van der Does, C.; Swaving, J.; van Klompenburg, W.; Driessen, A. J. M. Non-bilayer Lipids Stimulate the Activity of the Reconstituted Bacterial Protein Translocase. *J. Biol. Chem.* **2000**, *275*, 2472−2478.
(13) Hamai, C.; Yang, T.; Kataoka, S.; Cremer, P. S.; Musser, S. M. Effect of Average Phospholipid Curvature on Supported Bilayer Formation on Glass by Vesicle Fusion. *Biophys. J.* **2006**, *90*, 1241−1248.
(14) Kollmitzer, B.; Heftberger, P.; Rappolt, M.; Pabst, G. Monolayer Spontaneous Curvature of Raft-Forming Membrane Lipids. *Soft Matter* **2013**, *9*, 10877−10884.
(15) Strandberg, E.; Tiltak, D.; Ehni, S.; Wadhwani, P.; Ulrich, A. S. Lipid shape is a key factor for membrane interactions of amphipathic helical peptides. *Biochim. Biophys. Acta, Biomembr.* **2012**, *1818*, 1764−1776.
(16) Sakuma, Y.; Imai, M. From Vesicles to Protocells: The Roles of Amphiphilic Molecules. *Life* **2015**, *5*, 651.
(17) Tate, M. W.; Eikenberry, E. F.; Turner, D. C.; Shyamsunder, E.; Gruner, S. M. Nonbilayer phases of membrane lipids. *Chem. Phys. Lipids* **1991**, *57*, 147−164.
(18) Koynova, R.; Caffrey, M. Phases and phase transitions of the hydrated phosphatidylethanolamines. *Chem. Phys. Lipids* **1994**, *69*, 1−34.
(19) Seddon, J. M.; Cevc, G.; Kaye, R. D.; Marsh, D. X-Ray Diffraction Study of the Polymorphism of Hydrated Diacyl and Dialkylphosphatidylethanolamines. *Biochemistry* **1984**, *23*, 2634−2644.
(20) McLaughlin, A.; Grathwohl, C.; McLaughlin, S. The Adsorption of Divalent Cations to Phosphatidylcholine Bilayer Membranes. *Biochim. Biophys. Acta* **1978**, *513*, 338−357.
(21) Hope, M. J.; Bally, M. B.; Webb, G.; Cullis, P. R. Production of large unilamellar vesicles by a rapid extrusion procedure. Characterization of size distribution, trapped volume and ability to maintain a membrane potential. *Biochim. Biophys. Acta* **1985**, *812*, 55−65.
(22) Mayer, L. D.; Hope, M. J.; Cullis, P. R. Vesicles of variable sizes produced by a rapid extrusion procedure. *Biochim. Biophys. Acta* **1986**, *858*, 161−168.
(23) Axelrod, D.; Koppel, D. E.; Schlessinger, J.; Elson, E.; Webb, W. W. Mobility Measurement by Analysis of Fluorescence Photobleaching Recovery Kinetics. *Biophys. J.* **1976**, *16*, 1055−1069.
(24) Soumpasis, D. M. Theoretical Analysis of Fluorescence Photobleaching Recovery Experiments. *Biophys. J.* **1983**, *41*, 95−97.
(25) Robison, A. D.; Huang, D.; Jung, H.; Cremer, P. S. Fluorescence modulation sensing of positively and negatively charged proteins on lipid bilayers. *Biointerphases* **2013**, *8*, 1.
(26) Cannon, B.; Hermansson, M.; Györke, S.; Somerharju, P.; Virtanen, J. A.; Cheng, K. H. Regulation of Calcium Channel Activity by Lipid Domain Formation in Planar Lipid Bilayers. *Biophys. J.* **2003**, *85*, 933−942.
(27) Bao, P.; Cheetham, M. R.; Roth, J. S.; Blakeston, A. C.; Bushby, R. J.; Evans, S. D. On-Chip Alternating Current Electrophoresis in Supported Lipid Bilayer Membranes. *Anal. Chem.* **2012**, *84*, 10702−10707.
(28) Callan-Jones, A.; Sorre, B.; Bassereau, P. Curvature-Driven Lipid Sorting in Biomembranes. *Cold Spring Harbor Perspect. Biol.* **2011**, *3*, a004648.
(29) Monson, C. F.; Cong, X.; Robison, A. D.; Pace, H. P.; Liu, C. M.; Poyton, M. F.; Cremer, P. S. Phosphatidylserine Reversibly Binds Cu^{2+} with Extremely High Affinity. *J. Am. Chem. Soc.* **2012**, *134*, 7773−7779.
(30) Cong, X.; Poyton, M. F.; Baxter, A. J.; Pullanchery, S.; Cremer, P. S. Unquenchable Surface Potential Dramatically Enhances Cu^{2+} Binding to Phosphatidylserine Lipids. *J. Am. Chem. Soc.* **2015**, *137*, 7785−7792.
(31) Irving, H.; Williams, R. J. P. Order of Stability of Metal Complexes. *Nature* **1948**, *162*, 746−747.
(32) Irving, H.; Williams, R. J. P. The Stability of Transition-metal Complexes. *J. Chem. Soc.* **1953**, 3192−3210.
(33) Gordon, S. E.; Senning, E. N.; Aman, T. K.; Zagotta, W. N. Transition metal ion FRET to measure short-range distances at the intracellular surface of the plasma membrane. *J. Gen. Physiol.* **2016**, *147*, 189−200.
(34) Anglin, T. C.; Conboy, J. C. Kinetics and Thermodynamics of Flip-Flop in Binary Phospholipid Membranes Measured by Sum-Frequency Vibrational Spectroscopy. *Biochemistry* **2009**, *48*, 10220−10234.
(35) Simonsson, L.; Höök, F. Formation and Diffusivity Characterization of Supported Lipid Bilayers with Complex Lipid Compositions. *Langmuir* **2012**, *28*, 10528−10533.
(36) Slater, S. J.; Ho, C.; Taddeo, F. J.; Kelly, M. B.; Stubbs, C. D. Contribution of Hydrogen Bonding to Lipid-Lipid Interactions in Membranes and the Role of Lipid Order: Effects of Cholesterol, Increased Phospholipid Unsaturation, and Ethanol. *Biochemistry* **1993**, *32*, 3714−3721.
(37) Murzyn, K.; Róg, T.; Pasenkiewicz-Gierula, M. Phosphatidylethanolamine-Phosphatidylglycerol Bilayer as a Model of the Inner Bacterial Membrane. *Biophys. J.* **2005**, *88*, 1091−1103.
(38) Jendrasiak, G. L. The hydration of phospholipids and its biological significance. *J. Nutr. Biochem.* **1996**, *7*, 599−609.
(39) Garidel, P.; Blume, A. Miscibility of phosphatidylethanolamine-phosphatidylglycerol mixtures as a function of pH and acyl chain length. *Eur. Biophys. J.* **2000**, *28*, 629−638.
(40) Seeger, H. M.; Marino, G.; Alessandrini, A.; Facci, P. Effect of Physical Parameters on the Main Phase Transition of Supported Lipid Bilayers. *Biophys. J.* **2009**, *97*, 1067−1076.
(41) Teixeira, V.; Feio, M. J.; Bastos, M. Role of lipids in the interaction of antimicrobial peptides with membranes. *Prog. Lipid Res.* **2012**, *51*, 149−177.
(42) Haney, E. F.; Nathoo, S.; Vogel, H. J.; Prenner, E. J. Induction of non-lamellar lipid phases by antimicrobial peptides: a potential link to mode of action. *Chem. Phys. Lipids* **2010**, *163*, 82−93.
(43) Arouri, A.; Dathe, M.; Blume, A. Peptide induced demixing in PG/PE lipid mixtures: A mechanism for the specificity of antimicrobial peptides towards bacterial membranes? *Biochim. Biophys. Acta, Biomembr.* **2009**, *1788*, 650−659.

DOI: 10.1021/acs.langmuir.7b02323
Langmuir 2017, 33, 13423−13429